CHAPTER 1

CHAPTER 1

Interfacial and Aggregation Behavior of Dicarboxylic Amino Acid Based Surfactants in Combination with a Cationic Surfactant

ABSTRACT

Interfacial and micellization behavior of three dicarboxylic amino acid based anionic surfactants (*N*-dodecyl derivatives of amino-malonate, -aspartate and -glutamate) in combination with hexadecyltrimethylammonium bromide (HTAB) were investigated by surface tension, conductance, UV-VIS absorption/emission spectroscopy, dynamic light scattering and viscosity studies. Critical micelle concentration (CMC) values of the surfactant mixtures were significantly lower than the predicted values, indicating strong synergistic interaction. Surface excess, limiting molecular area, surface pressure at the CMC and Gibbs free energy indicate spontaneity of the micellization processes, compared to the pure components. CMC values were also determined from the sigmoidal variation in the micellar polarity and pyrene UV-VIS absorbance/emission spectra with surfactant concentration. Aggregation number (n), determined by the static fluorescence quenching method, increased with decreasing molefraction of the anionic surfactants ($\alpha_{(C_{12}AAS)_2Na_2}$) because of the dominance of the HTAB molecules in micelle. Micellar size increased with decreasing $\alpha_{(C_{12}AAS)_2Na_2}$, leading to the formation of larger and complex aggregates. Micelles comprising 20 - 40 mole% (C_{12}AAS)Na_2 were highly viscous in consonance with their sizes. Some of the mixed surfactant systems showed unusual viscosity (shear thickening and increased viscosity with increasing temperature). Such mixed surfactant systems are considered to have potentials in gel-based drug delivery and nanoparticle synthesis.

***Langmuir*, 2019, 35 (47), 15306-15314**

DOI:10.1021/acs.langmuir.9b02895

1. INTRODUCTION

Self-aggregation behavior of mixed surfactant systems depend on its composition and environmental conditions like temperature, pressure, salinity and solvent nature.[2-5] They usually have lower critical micelle concentration (CMC) than the individual components, [156, 157] because of specific synergistic interactions.[158] Different kinds of interactions like adhesive/cohesive forces and hydrogen bonding, operative for such systems, result in the lower CMC values.[159] Reports on the investigations of mixed surfactants include cationic/anionic,[86] cationic/cationic,[160] cationic/nonionic,[161] anionic/nonionic[162] and zwitterionic/anionic[163] systems, to mention a few. Oppositely-charged mixed surfactants, through electrostatic attraction, form a variety of aggregates depending on the chain length of the mixed surfactants.[2, 4, 85, 164-170] Equimolar mixtures of oppositely charged surfactants in aqueous medium form ion pair amphiphile (IPA), also known as coacervates, as they quite often precipitate out.[4, 70, 85, 166, 171-174] An IPA usually contains two hydrocarbon chains; where the two alkyl chains are non-covalently attached while electrostatic interaction occurs between the oppositely charged head groups,[70] that facilitates the process of aggregation. Electrostatic interactions between the two oppositely charged head groups result in different hydration energy of the surfactant mixtures compared to the individual surfactant.[70, 85, 166, 171, 172, 174] Oppositely charged mixed surfactant systems are capable to achieve higher surface activity and lower CMC compare to the surfactant individually.[168] Studies involving bivalent anionic surfactants, for example, the presently investigated *N*-dodecyl derivatives of amino-malonate, -aspartate and -glutamate (C_{12}AAS)Na_2 in combination with a cationic surfactant hexadecyltrimethylammonium bromide (HTAB) are not common in the literature. Oppositely charged mixed surfactants mainly form micelles and vesicles in aqueous medium; the di-anionic groups are dominant factors in regulating these unique aggregation behavior.[165] With a slight excess of either of the surfactants, it is quite common to experience the formation of vesicle. The surface ionic charge from the excess surfactant is shielded / screened by two factors: i) charge neutralization and ii) presence of excess salt, produced from the counter ions of the two surfactants.[175] In case of cationic-anionic mixed surfactant systems, micellar aggregation number are

substantially high, so the systems can form stable vesicles without the need for highly energetic methods such as sonication and extrusion.[176] In general, mixed surfactant systems demonstrate various complex phases.[177] Precipitation, coacervation,[178] and liquid crystal formation,[121] arise at extremely low surfactant concentration. Appearance of different phases or liquid crystals in case of mixed surfactants sturdily depend on the composition, the relative number of alkyl chains per surfactant, temperature and salinity, *etc*.[5] It is expected that the presently studied oppositely charged mixed surfactant systems would exhibit synergistic interaction,[44,179] thus minimizing the need of the individual surfactant components. Conventional single tail anionic surfactants, *viz.*, sodium dodecylsulphate (SDS) and sodium deoxycholate (NaDC) have limitations as they can break the C and N terminal peptide bonds that prevent the DNA translocation, unlike the $(C_{12}AAS)Na_2$.[180] HTAB is substantially toxic for human; so its uses can be avoided by combining it with the $(C_{12}AAS)Na_2$ where it is expected that the individual toxicities/ intolerances could substantially be minimized. Higher hydrophilicity of $(C_{12}AAS)Na_2$ are significantly different from the corresponding amino acids. Hence the influence of chain length on the aggregation behavior of such surfactants in combination with HTAB is considered to be important.

The present study intends to investigate the relatively more complex systems: formation of binary aggregates between amino acid based surfactants ($C_{12}MalNa_2$, $C_{12}AspNa_2$ and $C_{12}GluNa_2$) and a cationic surfactant HTAB. HTAB is well known for its multifaceted applications like fabrication of nonmaterial, [181] drug delivery,[182] cell lysis,[183] microemulsion formulation,[184] molecular separation,[15] biochemical research,[185] lubrication,[186] and cleaning operations,[89] to mention a few. AASs is capable of forming vesicles, for which it shows manifold applications in biological systems, emulsification,[23] foaming control, surfactant-based separation, surface wetting modification and flotation.[24]

Another point of interest in the current system is the structural heterogeneities between the two surfactants. The $(C_{12}AAS)Na_2$ have one dodecyl chain while HTAB comprises a hexadecyl chain. The second difference between the $(C_{12}AAS)Na_2$ and HTAB lies in the charge of the surfactant head groups.

Due to the difference in alky chain length, the presently investigated systems are less likely to form precipitate at stoichiometric ratio, as quite common in other conventional binary surfactant mixtures.[14] Most importantly the anionic surfactants studied herein, include *N*-dodecyl amino -malonate, -aspartate and -glutamate where the two carboxylic acid moieties are progressively separated by methylene group. Thus, it is expected that the structural differences will lead to asymmetry which in turn, would produce complex assemblies. This could have profound effects on the viscosity of the aggregates.

Interfacial and micellar aggregation behavior of mixed surfactants system were investigated by different experimental techniques such as electrical conductance, surface tension, UV-Vis absorbance/emission spectroscopy, dynamic light scattering (DLS) and viscosity measurements. Different physicochemical parameters, *viz*. critical micelle concentration (CMC), surface excess (Γ_{max}), surface pressure at CMC (π_{CMC}), number of molecules per unit area (A_{min}), Gibbs free energy of micellization (ΔG^0_{mic}), interfacial adsorption (ΔG^0_{ads}), fraction of counter ion binding (β), hydrodynamic diameter (d_h), polydispersity index (PDI), aggregation number (n) and zero shear viscosity (η_0) values were evaluated. Influence of counter-ion specificity is vital for the surface activity of an amphiphile. Dicarboxylic (C_{12}AAS)Na_2 are potential chelating agents for mono- and divalent cations. Two carboxylate head groups come in close contact with each other and one adjacent amide bond is known to exhibit the metal chelating properties.[187] (C_{12}AAS)Na_2 are not only environmentally benign, but also display different specific characters of carboxylic polar head groups.

Till date, no comprehensive studies on mixed surfactants are available in the literatures that include (C_{12}AAS)Na_2 as one of the components. As (C_{12}AAS)Na_2 contain two anionic carboxylic acid groups, they do not interact prominently with the HTAB, because during hydration, polar head groups of (C_{12}AAS)Na_2 interact with water molecule so (C_{12}AAS)Na_2 alone cannot be considered as a suitable candidate for the formation of micelles, where low CMCs are warranted. It is believed that the studies on

the interfacial and aggregation behavior of such binary surfactants can provide new insights, that will eventually help in understanding the bulk and interfacial activities of mixed surfactant systems.

2. EXPERIMENTAL SECTION

2.1. ***Materials.*** Hexadecyltrimethylammonium bromide (HTAB), hexadecylpyridinium chloride (HPC), lauroyl chloride, L-aspartic acid, L-glutamic acid, *N*-acetyl-L-glutamic acid, L-glycine ethyl ester, terahydrofuran (THF) anhydrous and pyrene were the products from Sigma-Aldrich Chemicals Pvt. Ltd. (USA). Aminomalonic acid diethyl ester hydrochloride, *N*-acetyl-L- aspartic acid, hydrochloric acid and sodium hydroxide were purchased from Fluka (Germany). (C_{12}AAS)Na_2 were synthesized and purified which was discussed in (supporting information).[25, 124] Double distilled water with specific conductance 2-4 μS at 298 K was used throughout the experiments. All the chemicals were stated to be ≥ 99% pure and were used as received. Structures of HTAB and the newly synthesized surfactants are shown in Scheme 1.

Sodium *N*-dodecyl aminomalonate (C_{12}MalNa_2) Sodium *N*-dodecyl aminoaspartate (C_{12}AspNa_2)

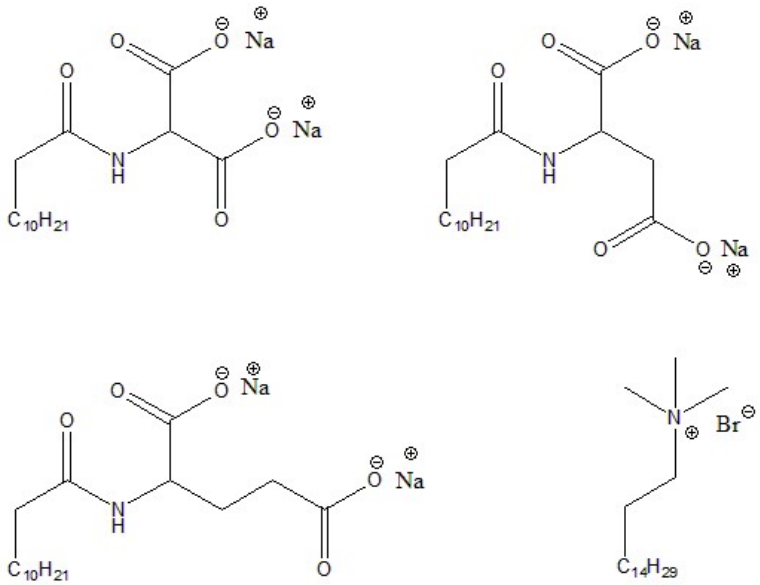

Sodium *N*-dodecyl aminoglutamate (C_{12}GluNa_2) Hexadecyltrimethylammonium bromide (HTAB)

Scheme 1. Chemical structure of the surfactants.

2.2.Methods.

2.2.1. ***Determination of critical micelle concentration (CMC).*** The CMC value of the pure as well as mixed surfactants was determined by surface tension, conductance, UV-VIS absorption/emission spectroscopic techniques.

2.2.2. ***Surface tension studies:*** Twenty times (anticipated, or literature value of the *CMC*) concentrated surfactant solutions were used as stock to perform the surface tension studies. At first, 20 ml water was taken in a jacketed container at controlled temperature (298 K). The temperature during the surface tension measurements were 298 K using a circulating water bath (Hanntech Corporation, South Korea). Water bath connected to a jacket container by the inlet and outlet port. At a controlled temperature (298K) water was flowing into the jacket container by inlet part and rejected by the outlet part and this process was circulated continuously during the surface tension experiment. The quantitative amount of surfactant stock solution was then progressively added into the water. It was then homogenized using a magnetic stirrer. After a 3 min of equilibration, surface tension of the solution was recorded by a du Noüy tensiometer with an accuracy of 0.1 mNm^{-1} (Jencon, Kolkata, India). From the break point of the surface tension *vs. log*C (surfactant concentration) plot, *CMC* value was determined.

2.2.3. ***Conductance studies:*** Similar protocol, as adopted in the surface tension measurement, was followed for the conductance studies, where the conductance of the solution was recorded by a direct reading conductivity meter, Con 510 (Eutech Instruments, Singapore) with an accuracy of ±0.1 μS cm^{-1}. Conductance measurements were taken at a frequency of 1 kHz, using a dip-type conductance cell of 0.92 cm^{-1} cell constant. From the break point of the conductance *vs.* surfactant concentration plots, *CMC* values were determined.[88]

2.2.4. ***UV-VIS absorbance and emission spectroscopic studies.*** Pyrene was used as the probe for the UV-visible absorption and emission spectroscopy studies. Initially, a 1000μM pyrene solution was

prepared in ethanol and then it was further diluted to 100μM using ethanol. 2.0 μM pyrene (Py) solution in water was obtained by proper dilution and sonication for half an hour. Though the medium contained 0.5% (v/v) alcohol, it was considered to have little effect on the surfactant aggregation. Final 2μM pyrene solution-dispersion in water was within the solubility limit.[85] UV-VIS absorption spectra were recorded by a UV-VIS spectrophotometer (UVD-2950, Labomed Inc., USA). Pyrene exhibits three major absorption peaks at 242, 275 and 338 nm and four weak bands at 233, 253, 265 and 322 nm respectively, Figure 1.[188]

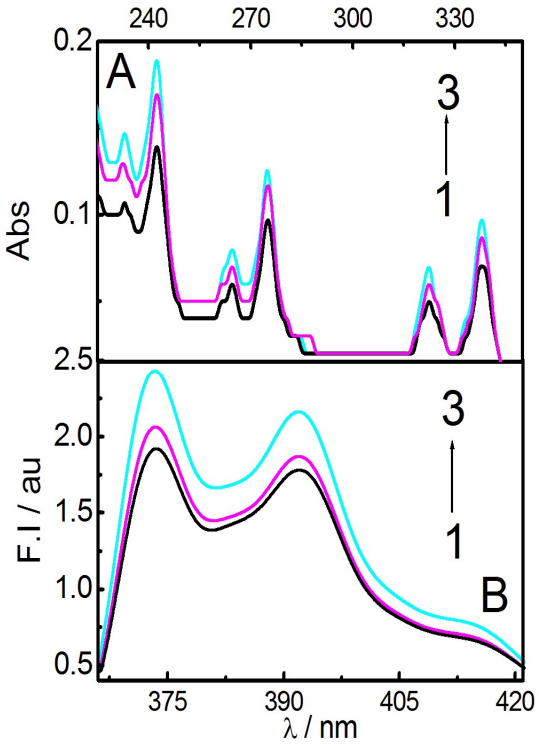

Figure 1. UV-vis absorption (panel A) and emission spectra (panel B) of 2.0 μM pyrene in presence of varying ($C_{12}GluNa_2$: HTAB, 4:1 M/M) concentration of surfactant. Surfactant concentration (mM): 1, 0.0189; 2, 0.038 and 3, 0.057. Temperature: 298 K.

Fluorescence spectroscopic studies were performed by a spectrofluorometer (Hitachi High Technologies Fluorescence Spectrophotometer Corporation, F-7100, TOKYO, Japan), where the first emission vibronic peak at 373 nm (I_1) and the third emission vibronic peak at 393 nm (I_3) respectively were considered. The emission spectra of pyrene in the presence of varying amount of surfactants have been shown in Figure 1, along with its absorption spectra. Four times concentrated (than the anticipated / reported *CMC* of surfactant) surfactant solutions were used as stock for UV-VIS absorption and emission spectroscopy

studies. In spectroscopic studies, 2mL aqueous pyrene solution was taken in a quartz cuvette, another cuvette filled with water was used as reference. The quantitative amount of surfactant solution, prepared in 2μM pyrene, was gradually added into experimental cuvette and was homogenized. Absorption spectra were recorded in the wavelength range 230 to 350 nm. The sum of the absorbance of all the major peaks / bands of pyrene (A_T) was plotted against the surfactant concentration. From the sigmoidal plot, the *CMC* value was calculated using the following expression:[48]

$$A_T = \frac{(a_i - a_f)}{\left[1+\exp^{\frac{(x-x_0)}{\Delta x}}\right]} + a_f \quad (1)$$

where, a_i and a_f are the initial and final asymptotes of the sigmoid respectively, x_0 is the center of the sigmoid (herein the *CMC*) and Δx is the interval of the independent variable x. Excitation wavelength of pyrene was set at 335 nm and emission spectra were recorded in the wavelength range of 350 to 550 nm. *CMC* value was also obtained from the sigmoidal curve, in the I_1/I_3 *vs.* [surfactant] plot. Aggregation number (n) of the surfactants was determined by fluorescence quenching method using pyrene as the probe and hexadecyl pyredinium chloride (HPC) as the quencher. [101]

2.2.5. Dynamic light scattering (DLS) studies. Hydrodynamic diameter (d_h) and polydispersity index (PDI) values of the surfactant aggregates were measured using a Zetasizer Nano ZS-90 (Malvern Instruments, U.K.) dynamic light scattering spectrometer. Solutions were filtered carefully through a 0.45 μm Millipore cellulose acetate membrane filter. He-Ne laser operating at 632.8 nm was used as the light source; scattering angle was set at 90°. Ten times concentrated surfactant solution than the corresponding CMC values were used for the DLS studies. Solution of higher concentration could not be used as those systems were highly viscous that interfered with the DLS studies.

2.2.6. Viscosity studies. Viscosity of surfactant solutions were measured by a DV II-Pro rotoviscometer (Brookfield, USA) with a stated accuracy of ±0.01 cP. Some mixed surfactant systems exhibited high viscosity; they formed different liquid crystals (as observed through polarization optical

microscope, data not shown). 1.0 ml surfactant solution (of different concentration: 50-150 mm) was taken in the cone and plate type rotoviscometer. Viscosity of pure as well as mixed surfactant systems were measured at different shear rates (ranging from 76 to 380 s^{-1}). Zero shear viscosity was determined from the intercept of the plot of viscosity *vs.* shear rate by fitting polynomial regression. Experiments were carried out in the temperature range of 288 to 318 K where the temperature was controlled by a circulatory water bath (Hanntech Corporation, South Korea).

All the experiments, unless otherwise stated, were carried out at 298 K.

3. RESULTS AND DISCUSSION

3.1. Critical micelle concentration (CMC). Representative surface tension (γ) *vs. log* [surfactant], specific conductance *vs.* [surfactant], A_T *vs.* [surfactant] and I_1/I_3 *vs.* [surfactant] plots are shown in Figure 2 where from the *CMC* values were determined. *CMC* of pure HTAB was 0.73 mM, close to the literature value.[85]

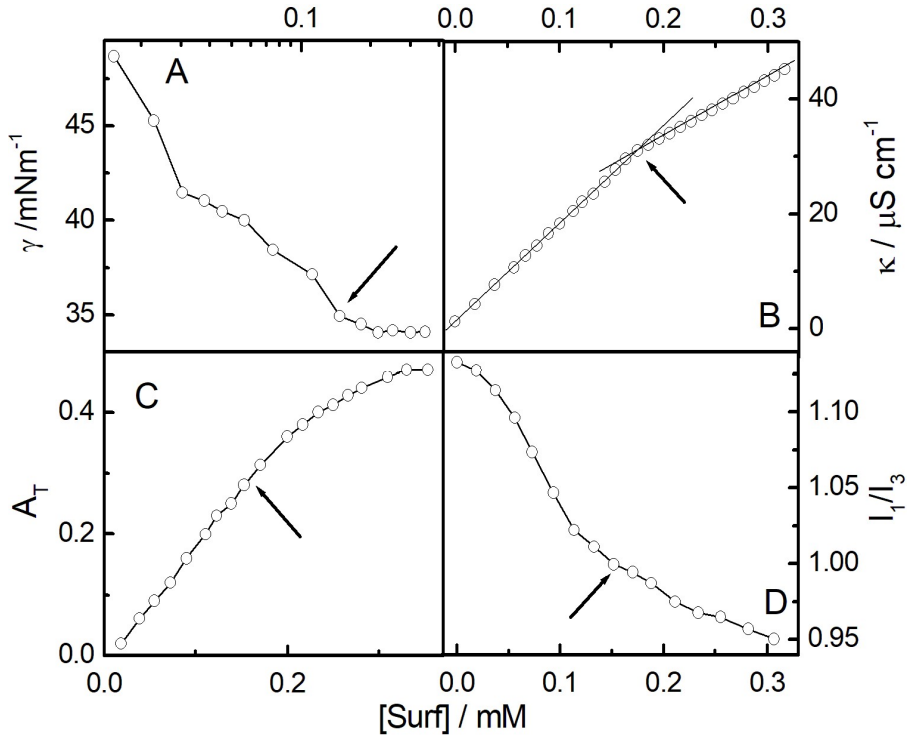

Figure 2. Variation of surface tension (γ), specific conductance (κ), sum of the peak absorbance (A_T) and I_1/I_3 ratio with surfactant concentration at 298 K. 4:1 (M/M) $C_{12}GluNa_2$ and HTAB mixed surfactant system was used. [Pyrene] = 2 μM. Excitation wavelength: 335 nm.

Table 1. Experimental CMC, surface pressure at CMC (π_{CMC}), surface excess (Γ_{max}), area minimum (A_{min}), Gibbs free energy of micellization (ΔG^0_{mic}), Gibbs energy change in interfacial adsorption (ΔG^0_{ads}), fraction of counter ion binding (β) and aggregation number (n) of $(C_{12}AAS)Na_2$ - HTAB mixed surfactant system at 298K.

$\chi_{(C_{12}AAS)_2Na_2}$	CMC/mM					π_{CMC}/ mNm^{-1}	$10^6\Gamma_{max}$ /mol m^{-2}	A_{min} / nm^2 molecule^{-1}	(-)ΔG^0_{mic} / kJ.mol^{-1}	(-)ΔG^0_{ads} / kJ.mol^{-1}	β	n
	Surface Tension	Cond.	Fluo. Spectro.	UV-VIS Abs.	Expt. Average (CMC_{av})							
HTAB-sodium *N*-dodecylaminomalonate												
1.0	44.82	50.87	53.85	55.12	51.20	34.4	1.86	0.88	27.59	66.88	0.52	37
0.8	0.15	0.15	0.16	0.14	0.15	40.9	1.68	0.98	43.68	68.88	0.35	32
0.6	0.09	0.09	0.10	0.08	0.09	40.9	1.67	0.99	41.47	67.54	0.23	48
0.5	0.06	0.06	0.11	0.06	0.07	42.2	1.85	0.89	46.68	68.33	0.37	50
0.4	0.06	0.06	0.08	0.04	0.06	43.1	1.52	1.09	53.24	81.57	0.53	55
0.2	0.04	0.04	0.05	0.03	0.04	41.5	1.57	1.05	55.45	81.87	0.58	63
0.0	0.72	0.73	0.75	0.72	0.73	32.6	0.90	1.84	49.58	85.81	0.77	65
HTAB-sodium *N*-dodecylaminoaspartate												
1.0	54.18	46.83	41.23	42.87	46.30	32.4	2.38	0.69	26.53	62.36	0.55	51
0.8	0.15	0.13	0.14	0.14	0.14	39.4	1.75	0.94	41.65	64.18	0.33	28
0.6	0.09	0.08	0.07	0.08	0.08	39.8	1.83	0.90	42.95	64.19	0.31	32
0.5	0.04	0.05	0.08	0.07	0.06	40.6	1.70	0.97	46.73	69.52	0.40	48
0.4	0.04	0.05	0.04	0.06	0.05	41.6	1.38	1.20	47.29	75.71	0.39	54
0.2	0.04	0.04	0.04	0.03	0.04	40.2	1.39	1.18	55.74	84.39	0.60	62
HTAB-sodium *N*-dodecylaminoglutamate												
1.0	33.81	36.67	40.28	35.03	36.45	31.2	2.30	0.71	28.12	56.81	0.60	49
0.8	0.17	0.15	0.07	0.09	0.12	37.5	1.50	1.07	41.43	66.22	0.28	32
0.6	0.06	0.08	0.06	0.07	0.07	39.6	1.72	0.96	45.83	69.98	0.35	35
0.5	0.05	0.06	0.04	0.05	0.05	39.5	1.59	1.04	46.48	71.36	0.35	44
0.4	0.04	0.05	0.04	0.04	0.04	40.3	1.30	1.27	59.00	90.04	0.60	48
0.2	0.03	0.04	0.03	0.03	0.03	39.2	1.27	1.30	57.71	88.61	0.65	56

CMC values of $C_{12}MalNa_2$, $C_{12}AspNa_2$ and $C_{12}GluNa_2$ were 51.2, 46.3 and 36.45 mM respectively, also comparable with the literature values.[25, 124] Results are summarized in Table 1 along with other data. With increasing mole fraction of the anionic surfactant $\alpha_{(C_{12}AAS)_2Na_2}$, CMC values gradually increased that follows the order: $C_{12}MalNa_2$+HTAB > $C_{12}AspNa_2$+HTAB > $C_{12}GluNa_2$+HTAB, Figure 3.

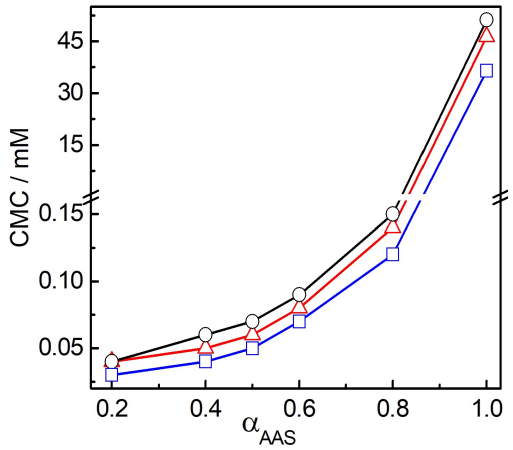

Figure 3. Variation of experimental *CMC* with the mole fraction of $(C_{12}AAS)Na_2$ ($\alpha_{(C_{12}AAS)_2Na_2}$) at 298 K. Systems: O, $C_{12}MalNa_2$-HTAB; Δ, $C_{12}AspNa_2$-HTAB and □, $C_{12}GluNa_2$-HTAB.

Higher CMC values of mixed surfactants system with increasing $\alpha_{(C_{12}AAS)_2Na_2}$, is a consequence of increasing hydrophobicity.[85, 88] CMC values of $(C_{12}AAS)Na_2$ were very much high and highly surface active, hence dianionic carboxylate of $(C_{12}AAS)Na_2$ closely interacted with HTAB and achieved higher CMC. Variation of CMC with the surfactant composition will be further discussed in detail in the subsequent section.

3.2. Interfacial behavior. Surface excess (Γ_{max}) of pure as well as mixed surfactants were calculated according to Gibbs formalism:[101]

$$\Gamma_{max} = -\frac{1}{2.303iRT}\frac{d\gamma}{d\log C} \quad (2)$$

where, C represents the surfactant concentration, 'i' is the Gibbs pre-factor, R and T have their usual significances. Γ_{max} is expressed in mol m^{-2} and i = 3 was used for the anionic surfactants while i = 2 was used for cationic surfactant. In case of mixed surfactant systems, the 'i' values were calculated on the

basis of relative proportion of the surfactants at different mole%. (C_{12}AAS)Na_2 homologs, as well as its mixtures with HTAB, were less surface active than HTAB. Hydrophobicity of (C_{12}AAS)Na_2 homologs were in accordance with its molecular weight, as also reflected through the Γ_{max} values. Incorporation of the methylene groups in between the two carboxylate anion would increase hydrophobicity of the (C_{12}AAS)Na_2. Γ_{max} *vs.* $\alpha_{(C_{12}AAS)_2Na_2}$ profiles are shown in Figure 4 (panel A).

The minimum area per surfactant molecule (A_{min}), is another parameter that can be evaluated as:[85]

$$A_{\min}(nm^2\text{molecule}^{-1}) = \frac{10^{18}}{N_A \Gamma_{\max}} \quad (3)$$

where, N_A is the Avogadro number. Surface pressure at CMC (π_{CMC}) values were calculated from the surface tension difference between pure water (γ_0) and the surfactant solution at its CMC (γ_{CMC}). π_{CMC} value of HTAB was 32.6 mNm^{-1}; for $C_{12}MalNa_2$, $C_{12}AspNa_2$ and $C_{12}GluNa_2$ they were 34.4, 32.4 and 31.2 mNm^{-1} respectively, as shown in Figure 4 (panel B). With increasing $\alpha_{(C_{12}AAS)_2Na_2}$, π_{CMC} values gradually decreased and passes through a minima due to the higher hydrophobic interaction between the oppositely charge surfactants. For all the mixed surfactant systems, π_{CMC} values were in the range between 37.5 to 43.1 mNm^{-1} (Table 1). π_{CMC} value depends on the CMC of the different surfactant mixtures. Two carboxylate anions of $C_{12}MalNa_2$ closely interact with HTAB in micelle than $C_{12}AspNa_2$ and $C_{12}GluNa_2$; hence π_{CMC} values follow the sequence $C_{12}MalNa_2$-HTAB > $C_{12}AspNa_2$-HTAB > $C_{12}GluNa_2$-HTAB. Γ_{max} values increased with increasing $\alpha_{(C_{12}AAS)_2M_2}$. Γ_{max} of HTAB molecule was 0.90 mol m^{-2}. For $C_{12}MalNa_2$, $C_{12}AspNa_2$ and $C_{12}GluNa_2$, Γ_{max} values were 1.86, 2.38 and 2.30 mol m^{-2} respectively (Table 1). All the values were close to the literature values.[25, 124] A_{min} values of (C_{12}AAS)Na_2 were lower than HTAB, thus for the mixed surfactants it was expected to decrease with the increasing proportion of the (C_{12}AAS)Na_2. Higher hydrophilicity of (C_{12}AAS)Na_2 molecules prefer to reside in the bulk water than at the interface compared to the HTAB.

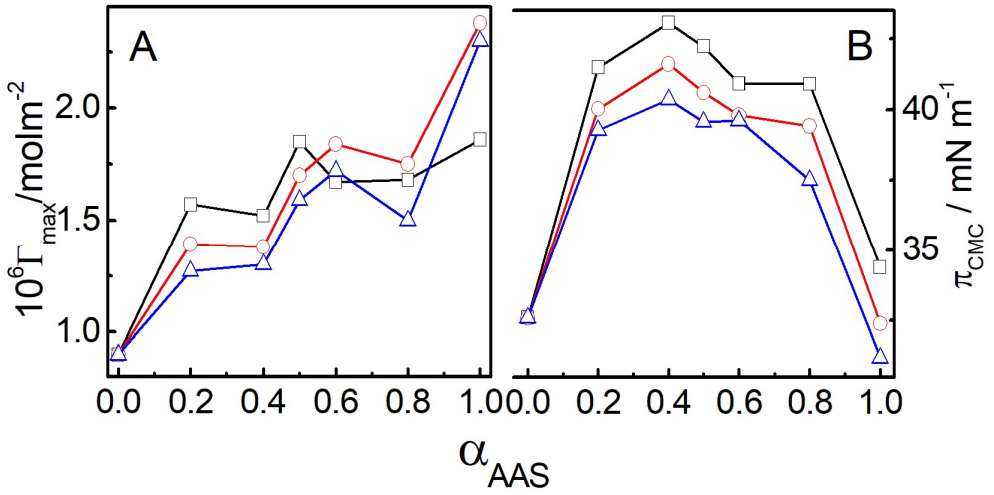

Figure 4. Variation surface excess (Γ_{max}) and surface pressure at CMC (π_{CMC}) with the mole fraction of $\alpha_{(C_{12}AAS)_2Na_2}$ at 298K. Systems: □, $C_{12}MalNa_2$- HTAB; O, $C_{12}AspNa_2$-HTAB; and Δ, $C_{12}GluNa_2$-HTAB.

The carboxylate groups get separated by methylene group(s); thus while moving from $C_{12}MalNa_2$, to $C_{12}AspNa_2$ to $C_{12}GluNa_2$, spacing between the two polar head groups gradually increases by one carbon atom sequentially. This leads to the increase in the hydrophobicity of the surfactants. In consonance with the increasing hydrophobicity, A_{min} values followed the sequence $C_{12}MalNa_2 > C_{12}AspNa_2 > C_{12}GluNa_2$. Higher A_{min} value of $C_{12}MalNa_2$-HTAB system implies the formation of close packed aggregate structure. Consequently, Γ_{max} values decreased and A_{min} value increased with increase in the $\alpha_{(C_{12}AAS)_2Na_2}$.

3.3. ***Conductance studies.*** CMC values were also determined from the break point of specific conductance (κ) *vs.* [surfactant] plot as shown in Figure 3 (panel B). Degree of counter ion dissociation (**α**) was calculated using the following equation: [88]

$$\boldsymbol{\alpha} = (S_2/S_1) \tag{4}$$

Where, S_1 and S_2 are the slopes of the pre- and post-micellar region in the specific conductance (κ) *vs.*[surfactant] plot respectively. Variation of '**α**' with $\alpha_{(C_{12}AAS)_2Na_2}$ are graphically shown in the Figure 5 (panel A). '**α**' value of HTAB was 0.23, [161] while for $C_{12}MalNa_2$, $C_{12}AspNa_2$ and $C_{12}GluNa_2$ it was 0.48, 0.45 and 0.40, respectively, close to the previously reported values. [25, 124] $(C_{12}AAS)Na_2$ molecules remain in more dissociated form than HTAB due to two carboxylate anions; the first dissociation takes away one

sodium ion that remains in solution as free ion. The second sodium ion coordinates with both the carboxylate anions stabilizing them that eventually promote higher mono dissociation of the $(C_{12}AAS)Na_2$.

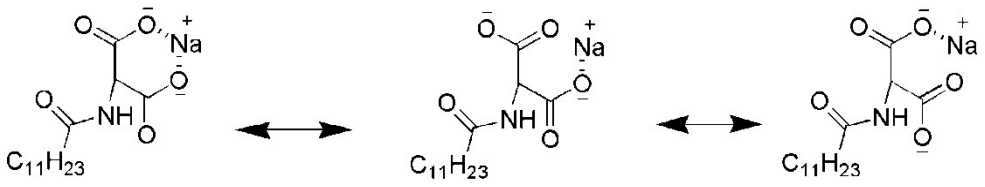

For $C_{12}MalNa_2$+HTAB mixture, with increasing mole % of $C_{12}MalNa_2$, '**α**' values gradually increased from 0.42 to 0.65. With increasing $\alpha_{(C_{12}AAS)_2Na_2}$, charge density increases on the micellar surfaces for which the 'α' value gradually increases which are also subsequently higher. For $(C_{12}AAS)Na_2$+HTAB mixture, with increasing $\alpha_{(C_{12}AAS)_2Na_2}$, '**α**' values pass through maxima because of the charge neutralization.

3.4. Thermodynamics of micellization. The change in the standard free energy of micellization (ΔG^0_{mic}) was calculated as :[88]

$$\Delta G^0_{mic} = (2-\boldsymbol{\alpha})\, RT\, ln\, X_{CMC} \quad (5)$$

Where, '**α**' is the fraction of counter ion dissociation, X_{CMC} is the CMC in the mole fraction scale. R and T have their usual meaning. Gibbs free energy of interfacial adsorption (ΔG^0_{ads}) was calculated as:[88]

$$\Delta G^0_{ads} = \Delta G^0_{mic} - \frac{\pi_{CMC}}{\Gamma_{max}} = \Delta G^0_{mic} - \frac{N_A \pi_{CMC}}{A_{min}} \quad (6)$$

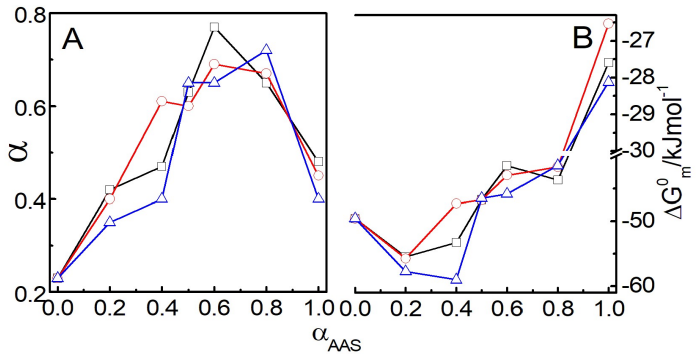

Figure 5. Variation of degree of dissociation (**α**) and free energy of micellization (ΔG^0_{mic}) with the molefraction of $(C_{12}AAS)Na_2$ $\alpha_{(C_{12}AAS)_2Na_2}$ at 298K. Systems: □, $C_{12}MalNa_2$-HTAB; O, $C_{12}AspNa_2$-HTAB and Δ, $C_{12}GluNa_2$-HTAB.

The negative value of ΔG^0_{mic}(-49.58 kJ.mol^{-1}) for HTAB was close to the literature value,[88] that indicates its spontaneity of micellization. For $C_{12}MalNa_2$-HTAB mixtures, with decreasing mole fraction of $C_{12}MalNa_2$ (α_{Mal}), the ΔG^0_{mic} values became, in general, more negative (-27.59 to -49.58 kJ mol^{-1}) which indicate further spontaneity of micellization and ΔG^0_{ads} (-61.88 to -85.81 kJ.mol^{-1}). Results are shown in Table 1. Magnitude of the negative ΔG^0_{mic} values of $(C_{12}AAS)Na_2$-HTAB mixtures decreased from -26.53 to -55.74 kJ mol^{-1} for aspartate and -28.12 to -57.71 kJ mol^{-1} for glutamate systems with decreasing molefraction of $(C_{12}AAS)Na_2$ ($\alpha_{(C_{12}AAS)_2Na_2}$) as shown in Figure 5 (panel B). It was also noted from conductance data that with the increasing $\alpha_{(C_{12}AAS)_2Na_2}$, maximum number of surfactant molecules are dissociated, thus the polarity of the medium increased. In case of mixed micelles, charge neutralization occurs among the oppositely charged surfactants; besides, the free counter ions further increase the polarity of the medium that make the micellization process more favorable.

3.5. Micellar aggregation number. Micellar aggregation number (n) was calculated using the following equation:[85]

$$ln\frac{I_0}{I} = \frac{n[Q]}{[S]-CMC} \quad (7)$$

where, I_0 and I represent fluorescence intensity of the probe in absence and presence of quencher (Q, HPC). [Q] is the quencher concentration and [S] is the total surfactant concentration. Aggregation number of HTAB was found to be 65, comparable with the literature value. [161] While for $C_{12}MalNa_2$, $C_{12}AspNa_2$ and $C_{12}GluNa_2$ they were 37, 51 and 49 respectively. Results are shown Table 1. For pure as well as mixed surfactant systems, experimentally observed aggregation numbers were in accordance with the micellar composition. With increasing the mole fraction of $\alpha_{(C_{12}AAS)_2Na_2}$, 'n' values gradually decreased. Mixed micelle contains larger proportion of HTAB molecules because of its smaller size; hence HTAB mainly dominate the micellar aggregation.[48,85] Third vibronic emission peak of pyrene (393 nm) was considered in determining the aggregation number (n). $ln(\frac{I_0}{I})$ *vs.* quencher concentration ([Q]) plots are shown in Figure 6.

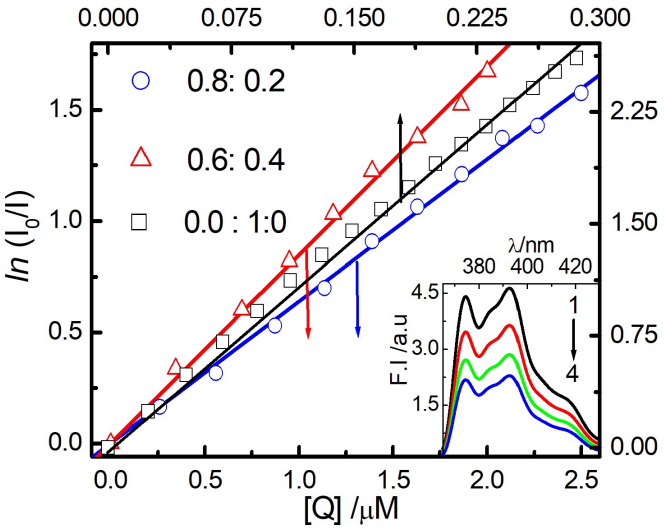

Figure 6. Plot of *ln*(I_o/I) with the quencher concentration [Q], (hexadecylpyridinium chloride, HPC) to determine the aggregation number of $C_{12}GluNa_2$-HTAB mixed surfactants at 298K. $C_{12}GluNa_2$ / HTAB ratio (M/M): □, 0.0: 1.0; O, 0.4: 0.1; and Δ, 0.3: 0.2. Inset: fluorescence spectra of pyrene (2.0μM) in the presence of varying concentration of HPC (μM): 1, 0.26; 2, 0.56; 3, 0.88 and 4, 1.13.

The hydrophobic interaction and accumulative cross sectional area of mixed surfactant systems are the main driving forces for the formation of larger and complex aggregates. Two anionic carboxylate groups of $(C_{12}AAS)Na_2$ repel each other that eventually results in the formation of larger aggregates. DLS studies also show that the size of the aggregates increased further supporting the increased aggregation number for the mixed surfactant systems.

3.6. Dynamic light scattering (DLS) studies. Size and polydispersity index (PDI) values of surfactant-aggregates were determined by DLS studies. d_h value of $C_{12}MalNa_2$, $C_{12}AspNa_2$ and $C_{12}GluNa_2$ were 2.2, 2.8 and 3.6 nm respectively. Initially, one of the two carboxylate groups of $(C_{12}AAS)Na_2$ undergoes dissociation; the remaining second sodium ion coordinates both the carboxylate groups to form six, seven and eight member cyclic conjugated rings in $C_{12}MalNa_2$, $C_{12}AspNa_2$ and $C_{12}GluNa_2$, respectively, as discussed previously. The hydrodynamic diameter (d_h) of HTAB molecule was 1.2 nm, close to the literature value as shown Figure 7 (panel A).[85]

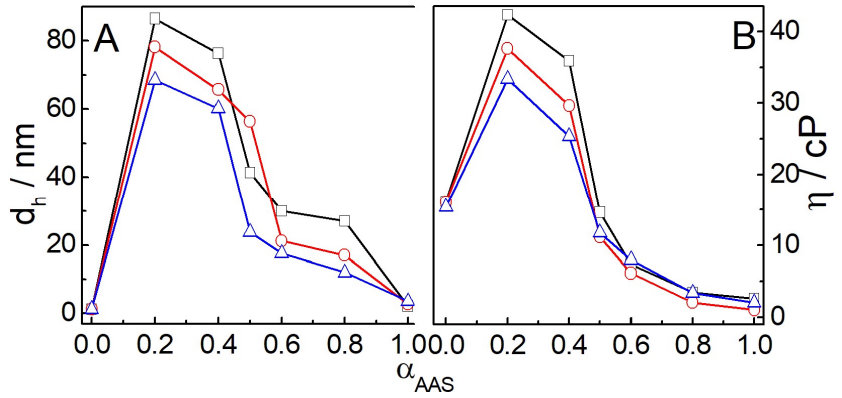

Figure 7. Variation of hydrodynamic diameter (d_h) and viscosity (η) with the molefraction of $(C_{12}AAS)Na_2$ ($\alpha_{(C_{12}AAS)_2Na_2}$) at 298 K. Systems: □, $C_{12}MalNa_2$-HTAB; O, $C_{12}AspNa_2$-HTAB; Δ, $C_{12}GluNa_2$-HTAB.

With increasing $\alpha_{(C_{12}AAS)_2Na_2}$, size of the mixed micelles gradually decreased as summarized in Table 2.

Table 2. Hydrodynamic diameter (d_h), polydispersity index (PDI) and zero shear viscosity (η_0) values at different molefraction of $(C_{12}AAS)Na_2$ ($\alpha_{(C_{12}AAS)_2Na_2}$), in $(C_{12}AAS)Na_2$-HTAB mixed surfactant systems at 298K.

$\alpha_{(C_{12}AAS)_2Na_2}$	d_h / nm	PDI	η_0
HTAB-malonate			
1.0	2.20	0.46	1.38
0.8	27.0	0.64	2.30
0.6	30.0	0.38	4.60
0.5	41.5	0.41	23.3
0.4	76.4	0.29	60.2
0.2	86.5	0.45	71.5
0.0	1.30	0.27	18.5
HTAB-aspartate			
1.0	2.80	0.46	1.71
0.8	17.0	0.61	1.29
0.6	21.2	0.54	3.40
0.5	56.4	0.39	19.0
0.4	65.8	0.30	58.6
0.2	78.2	0.46	64.4
HTAB-glutamate			
1.0	3.60	0.38	5.70
0.8	12.0	0.38	0.60
0.6	17.7	0.45	2.37
0.5	23.8	0.28	15.3
0.4	60.2	0.47	55.5
0.2	68.6	0.48	60.0

In the $(C_{12}AAS)Na_2$+HTAB mixed system, maximum number of HTAB molecules accumulated in the micelle which indicates that HTAB plays the fundamental role in exhibiting higher aggregation and enhancement of the size and it follow the sequence $C_{12}MalNa_2$+HTAB > $C_{12}AspNa_2$+HTAB > $C_{12}GluNa_2$+HTAB. In case of mixed micelles, the formation of less compact, yet rigid aggregates, results

in the size enhancement and this results correlate with miceller aggregation number and area minimum (A_{min}) in the micelle. Viscosity studies further support the proposition as will be discussed in the subsequent section. PDI value of HTAB was greater than 0.4 and the photon count rate was relatively low. However, for all the other systems, the PDI values were less than 0.6 and the count rates were substantially higher results are shown Table 2. Two major peaks were recorded at 3 and 25-30 nm for the mixed surfactant systems which that indicate, the formation of small micelles along with the larger aggregates.

3.7. Viscosity studies. (C_{12}AAS)Na_2 assorted with HTAB at different ratio were mainly viscous in nature. Viscosity *vs.* mole fraction of $\alpha_{(C_{12}AAS)_2Na_2}$ at a fixed shear rate profile are shown Figure 7 (panel B). Viscosities decreased with shear rate indicate thixotrophic behavior of the aggregates. (C_{12}AAS)Na_2 +HTAB mixed surfactants with 20 to 40 mol% (C_{12}AAS)Na_2 were highly viscous (gelatinous) that passed through maxima with increasing the $\alpha_{(C_{12}AAS)_2Na_2}$ and its also follows the sequence $C_{12}MalNa_2$+HTAB > $C_{12}AspNa_2$+HTAB > $C_{12}GluNa_2$+HTAB, indicating strong synergistic interaction. Carboxylate groups of (C_{12}AAS)Na_2 are separated by methylene groups, thus while moving from $C_{12}MalNa_2$, to $C_{12}AspNa_2$ to $C_{12}GluNa_2$, distance between two polar head groups gradually increases by one carbon atom sequentially. In consonance with the increasing hydrophobic force of interaction between the two oppositely charged head group followed the sequence: $C_{12}MalNa_2$-HTAB > $C_{12}AspNa_2$-HTAB > $C_{12}GluNa_2$-HTAB. It is proposed that during rotation, surfactant molecules get oriented to perpendicular direction to form vertical angle with respect to the rheological plate and accomplish entanglement efficiency. Initially viscosity sharply increased up to particular point with increasing shear rate up to 97 s^{-1}, then gradually decreased due to the shear thinning where entanglement effects are over powered by the rotational drags, even to zero.[189] In case of $C_{12}GluNa_2$-HTAB mixtures, for 40 mole% $C_{12}GluNa_2$, viscosity increased with increasing temperature. Such an unusual phenomenon was due to the formation of worm like micelle that led to the viscoelasticity probably contributed by the larger and complex aggregates in this temperature range. $C_{12}GluNa_2$-HTAB mixture was fashioned (a bit) to disordered aggregates and the aggregate

ordering stopped at a certain stage due to the kinetic reason. This is because the solution already becomes fluid through the rearrangement of the chains; however, this is even more ordered layer and hence is even more viscous. The second maximum with 40 mole% $(C_{12}AAS)Na_2$ in viscosity *vs.* $\alpha_{(C_{12}AAS)_2Na_2}$ was even higher, probably contributed by higher aggregation number of HTAB as the polar head group of HTAB closely interacts in the micelle. The results are well correlated with the DLS studies. Zero shear viscosity (η_0) *vs.* $\alpha_{(C_{12}AAS)_2Na_2}$ profiles for the three different surfactants mixtures are shown Figure 8. With increasing $\alpha_{(C_{12}AAS)_2Na_2}$, zero shear viscosity decreased where the decrease profiles obey two-degree polynomial fit with regression coefficient values close to 0.99, results are shown Table 2.

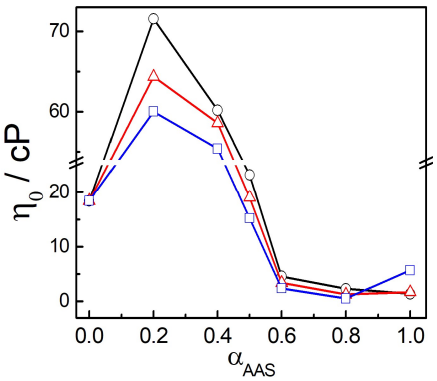

Figure 8. Variations of zero shear viscosity $(\eta_0)$with $\alpha_{(C_{12}AAS)_2Na_2}$. Systems: ○, $C_{12}MalNa_2$-HTAB; Δ, $C_{12}AspNa_2$-HTAB and □, $C_{12}GluNa_2$-HTAB. 150 mM surfactant solutions at 298 K were used.

In case of $(C_{12}AAS)Na_2$+HTAB mixed systems, particularly with 20-40 mole % of $(C_{12}AAS)Na_2$, higher zero shear viscosity values indicate the formation of larger spherical aggregates, as they were mainly highly viscous and even in the gel states. Initially, a three-fold increase in the zero shear viscosity value was noted. The aggregation number of $C_{12}MalNa_2$, $C_{12}AspNa_2$ and $C_{12}GluNa_2$ were 37, 51 and 49 respectively. This was due to the presence of lesser number of AASs molecules in the micelle where more fluid like entities were probable.[189] Thus, it could be concluded that, strong electrostatic interaction among the oppositely charged surfactants results in the formation of viscous or gel like materials. However, further structural investigations on the formation of liquid crystals or gel network, through the phase contrast microscopy, polarization optical microscopy (POM), fluorescence microscopy (FM), electron microscopy (SEM) and small-angle X-ray scattering (SAXS) are warranted. These are considered to be the future perspectives.

4. CONCLUSIONS

Interfacial and micellization behavior of $(C_{12}AAS)Na_2$-HTAB mixtures were studied using different physicochemical techniques. CMC values gradually increased with increasing proportion of $(C_{12}AAS)Na_2$, indicating increased hydrophobicity between the oppositely charged surfactants.[88] Negative Gibbs free energy of micellization indicates the spontaneity of the micellization process.[101] With increasing the mol % of $\alpha_{(C_{12}AAS)_2Na_2}$, surface pressure at the CMC (π_{CMC}) passes through minima due to strong synergestic interaction of surfactant mixtures. Oppositely-charged surfactants can achieve proximities to each other through the head group interaction and interact mainly at the micellar surface. Limiting molecular area of the mixed surfactant systems at the air-liquid interface gradually decreased and the surface excess values increased with increasing $\alpha_{(C_{12}AAS)_2Na_2}$.[166] Conductance studies showed that maximum numbers of the surfactant molecules are in their dissociated forms near the CMC; so the micellar surface charge density is higher. Micellar size gradually increased with decreasing $\alpha_{(C_{12}AAS)_2Na_2}$, due to the HTAB accumulated in the micelle.[48, 88] Rheological studies provide additional information on the internal structure of mixed surfactant aggregates. During micellization, maximum number of HTAB molecules cooperate on the micellar surface leading to the formation of closed packed aggregate structures.[85] Oppositely charged surfactants in their mixed states can form different viscous and gelatinous entities.[189] Viscosity studies reveal thixotropic nature of the mixed surfactant systems where viscosity did not change spontaneously with increasing the $\alpha_{(C_{12}AAS)_2Na_2}$, with few exceptions. Surfactant mixtures formed different types of aggregates; so the knowledge on the surface morphology by phase contrast,[121] polarization optical microscopic (POM),[190] fluorescence microscopic (FM),[191] and field emission scanning electronic microscopy (FE-SEM)[192] studies are considered to be essential, as will be carried out in future. Studies on the interfacial and micellization behavior of mixed surfactants are expected to provide new insights and can be used as drug delivery systems,[182] especially in dermatological formulations and to synthesize otherwise water insoluble inorganic nanoparticles.[193]